International Journal of Applied Mathematics, Sciences, and Technology for National Defense
Volume 4, Issue 2, 155-168
e_ISSN: 2985-9352, p_ISSN: 2986-0776
https://www.journal.foundae.com/index.php/JAS-ND
DOI : https://doi.org/10.58524/app.sci.def.v4i2.1274

Liquefaction potential and post-seismic volumetric strain of coastal deposits in Southern West Sumatera: A CPT and finite element approach for coastal defense infrastructure resilience

Okri Asfino Putra*
Indonesia Defense University
INDONESIA

Hamdeni Medriosa
Padang Institute of Technology
INDONESIA

Fajar Nugroho
Padang Institute of Technology
INDONESIA

Article Info

Article history:

Received: May 16, 2026
Revised: July 6, 2026
Accepted: August 4, 2026

Keywords:

Cone penetration test
Cyclic stress ratio
Liquefaction potential
Safety factor
West Sumatera

Abstract

Background: Previous liquefaction studies along the West Sumatera coast have mainly focused on the Padang urban area and have relied on triggering analysis using CSR–CRR. However, post-liquefaction ground deformation, which can affect coastal defense infrastructure, has received limited attention. This study addresses this gap by combining CPT-based liquefaction analysis with finite element modelling to estimate post-liquefaction ground settlement in the southern coastal segment. The results provide a quantitative basis for assessing liquefaction-induced deformation and supporting coastal infrastructure design in this earthquake-prone area.
Aims: Liquefaction is a major geotechnical hazard in coastal areas exposed to strong earthquakes, especially where loose and saturated sandy soils are present. The southern coast of West Sumatera is vulnerable to earthquake-induced liquefaction due to its proximity to the active Sunda megathrust. This study evaluates the liquefaction potential of coastal soils using Cone Penetration Test (CPT)-based analysis under different seismic loading conditions. Three CPT points were analyzed to characterize the subsurface soil and assess its liquefaction susceptibility.
Method: The liquefaction assessment compared the Cyclic Stress Ratio (CSR) from earthquake loading with the Cyclic Resistance Ratio (CRR) from CPT data. Peak ground accelerations of 0.15 g, 0.28 g, and 0.60 g were used to represent low, moderate, and strong earthquakes. The factor of safety (SF) was then calculated to identify soil layers susceptible to liquefaction. In addition, PLAXIS 2D was used to simulate post-liquefaction behavior using the Mohr–Coulomb model and CPT-based soil parameters, with the groundwater table set at 1.5 m depth. The analysis focused on the relationship between liquefaction resistance and post-liquefaction volumetric strain.
Result: The results show that liquefaction susceptibility increases with seismic intensity. At 0.15 g, most soil layers have SF values above 1.0 (1.2–3.8), indicating stable conditions. At 0.28 g, some layers at depths of 6–10 m become marginally unstable. At 0.60 g, most layers between 3 and 15 m have SF values below 1.0, indicating high liquefaction potential. The finite element results also show an inverse relationship between safety factors and volumetric strain ($R^2 = 0.78$), indicating that lower liquefaction resistance leads to greater post-liquefaction deformation.
Conclusion: Overall, this study demonstrates that the investigated coastal deposits are highly vulnerable to strong earthquake loading and emphasizes the importance of liquefaction mitigation measures for infrastructure development in earthquake-prone coastal regions.

To cite this article: Putra, O. A., Medriosa, H., & Nugroho, F. (2026). Liquefaction potential and post-seismic volumetric strain of coastal deposits in Southern West Sumatera: A CPT and finite element approach for coastal defense infrastructure resilience. *International Journal of Applied Mathematics, Sciences, and Technology for National Defense,* 4(2), 155-168.

***Corresponding Author:**
Okri Asfino Putra, Indonesia Defense University, Indonesia, Email: okri.putra@idu.ac.id

INTRODUCTION

The western coastal corridor of Sumatera Island represents one of the most tectonically active regions in Southeast Asia due to its direct interaction with the Sunda subduction system. The convergence between the Indo-Australian Plate and the Eurasian Plate continuously generates significant seismic activity, exposing coastal regions of West Sumatera to severe earthquake hazards (Tohari. A, 2020; Natawidjaja & Triyoso, 2007; Sieh & Natawidjaja, 2000). Several destructive earthquakes that occurred in this region have demonstrated the vulnerability of coastal infrastructure to seismic-induced ground failures, including soil liquefaction phenomena. The 2009 West Sumatera earthquake, for example, caused widespread geotechnical damage in coastal settlements and highlighted the necessity of evaluating subsurface stability in areas dominated by saturated granular deposits (Mase. L, 2017).

Coastal environments in southern West Sumatera are generally composed of young alluvial and marine sediments characterized by loose sand, silty sand, and shallow groundwater conditions. These geological characteristics significantly increase the susceptibility of the soil to earthquake-induced liquefaction. During seismic shaking, cyclic loading may generate excessive pore water pressure within saturated granular soils, reducing the effective stress and causing a temporary loss of shear strength. Under such conditions, the soil can behave similarly to a viscous fluid, resulting in settlement, bearing capacity failure, lateral spreading, and deformation of engineering structures (Boulanger et al, 2014; Tokimatsu et al, 1987; Tohwata. I, 2008; Yegian et al, 1981; Youd et al, 2001; Idris et al, 2018; Ishikara, 1993; Putra et al, 2014; Bray et al, 2006; Cetin et al, 2004; Das et al, 2018; Iwasaki et al., 1978; Seed et al., 1985)

Several in-situ investigation techniques have been adopted for liquefaction evaluation, including the Standard Penetration Test (SPT), shear wave velocity measurements, and Cone Penetration Test (CPT). Among these approaches, CPT has become widely accepted for liquefaction assessment because it provides continuous subsurface profiling with relatively high accuracy and repeatability. Cone resistance and sleeve friction measurements obtained from CPT investigations can be used to characterize soil behavior, estimate relative density, and evaluate liquefaction resistance of granular deposits. In addition, CPT investigations are relatively efficient for coastal environments because they can be conducted rapidly and produce detailed vertical soil profiles (Hall. R, 2012; Kramer. L, 1996; Lunne et al, 1997; Moss et al, 2006; Robertson et al, 2022; Seed et al, 1971; Seed et al, 2003; Robertson, 2009; Zhang et al., 2002; Andrus & Stokoe, 2000).

Previous liquefaction studies in West Sumatra have mainly concentrated on the Padang urban area, while detailed investigations along the southern coastal region remain relatively limited (Mase. L, 2017; Tohari. A, 2020). This lack of detailed subsurface information creates uncertainty in evaluating seismic hazards for future coastal infrastructure development. Considering the geological similarity between Padang coastal deposits and the southern coastal region of West Sumatra, there is a strong possibility that liquefaction-prone layers are also widely distributed in this area.

Most existing CPT-based liquefaction studies in this region, including those of (Mase. L, 2017; Tohari. A, 2020), evaluate only the triggering condition through the safety factor, and stop short of quantifying the resulting ground deformation. This limits their direct usefulness for infrastructure and coastal-defense design, where the magnitude of expected settlement, not merely the binary occurrence of liquefaction, governs engineering decisions. More recent international work has sought to address related uncertainties: (Boulanger and Idriss, 2016) refined the CPT-based triggering procedure itself; (Wang et al, 2023) quantified model uncertainties across SPT-, CPT-, and shear-wave-velocity-based simplified methods; and probabilistic and machine-learning-assisted approaches have been proposed to better capture spatial variability and case-history uncertainty in liquefaction assessment (Geyin and Maurer, 2021). Earlier, (Idriss and Boulanger, 2006) had already refined the magnitude scaling and overburden correction factors underlying both SPT- and CPT-based triggering procedures, (Juang et al, 2006) proposed a first-order reliability method for probabilistic CPT-based liquefaction triggering analysis, (Kayen et al, 2013) developed shear-wave-velocity-based probabilistic and deterministic triggering procedures, and (Bray and Macedo, 2017) presented a simplified procedure for estimating liquefaction-induced building settlement that complements CPT-based triggering assessments. In parallel, effective-stress finite element analysis has increasingly been used to simulate post-liquefaction volumetric strain and settlement using

constitutive soil models, which the conventional CSR-CRR comparison alone cannot provide. Building on these developments, the present study integrates empirical CPT-based triggering analysis with finite element modelling of post-liquefaction volumetric strain, offering a more complete, deformation-based picture of liquefaction hazard for the southern West Sumatera coast than has previously been reported for this area.

Therefore, this study aims to evaluate the liquefaction susceptibility of coastal deposits in southern West Sumatra using CPT-based analysis under different earthquake loading scenarios. The investigation focuses on identifying vulnerable soil layers, comparing cyclic stress demand and cyclic resistance, and assessing the factor of safety against liquefaction. Furthermore, finite element analysis was performed to evaluate the relationship between liquefaction resistance and post-earthquake volumetric strain behavior. The results of this study are expected to provide technical information for seismic hazard mitigation and support earthquake-resistant infrastructure planning in coastal environments.

METHOD

Field investigations were carried out in the southern coastal region of West Sumatra, Indonesia. The investigated area is dominated by coastal alluvial deposits consisting of loose sand, silty sand, clayey silt, and unconsolidated marine sediments. Groundwater conditions in the study area are relatively shallow because of the close proximity to the shoreline. Such geological and hydrogeological conditions are commonly associated with high liquefaction susceptibility during strong earthquake events.

Three Cone Penetration Test (CPT) soundings were conducted along the coastal zone to represent the spatial variation of subsurface conditions. The locations of the CPT points were selected based on geomorphological characteristics, shoreline proximity, and planned infrastructure development areas. The CPT investigations produced continuous measurements of cone tip resistance (qc) and sleeve friction (fs), which were subsequently interpreted to identify soil stratigraphy and evaluate liquefaction resistance. The distribution of CPT investigation points within the study area is presented in Figure 1.

The evaluation of soil liquefaction potential in this reserach was conducted using Cone Penetration Test (CPT) data combined with Cyclic Stress Ratio (CSR) and Cyclic Stress Resistance to Liquefaction (CSRL) analysis. The methodology aims to identify subsurface layers susceptible to liquefaction under earthquake loading conditions.

The liquefaction mechanism occurs when saturated loose sandy soils experience cyclic loading during earthquakes, causing an increase in excess pore water pressure and a reduction in effective stress. When the effective stress decreases significantly, the soil loses its shear strength and behaves temporarily as a fluid-like material (Seed and Idriss, 1971; Idriss and Boulanger, 2008), and the resulting post-liquefaction reconsolidation governs the volumetric strain and ground settlement that develop after shaking ceases (Ishihara and Yoshimine, 1992).

The subsurface characterization was first obtained from CPT investigations. The CPT provides continuous profiles of cone tip resistance (qc), sleeve friction (fs), and soil behavior type with depth. These parameters are essential for estimating the density and liquefaction resistance of sandy deposits. According to (Robertson et al, 2022), CPT-based liquefaction assessment is considered one of the most reliable methods for evaluating liquefaction susceptibility in granular soils.

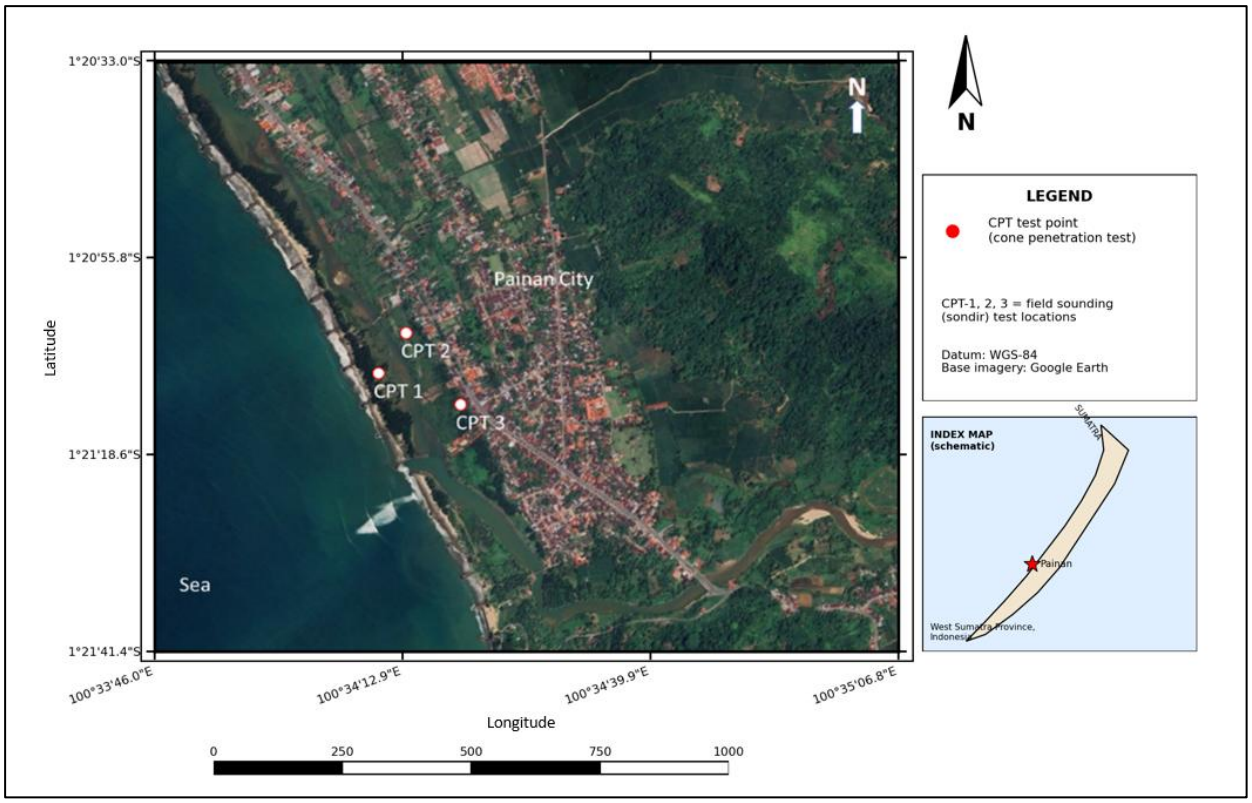


Figure 1. The CPT investigation location.

The earthquake-induced cyclic shear stress acting on soil layers was calculated using the simplified Seed and Idriss method:

$$CSR = 0.65 \left(\frac{a_{max}}{g}\right)\left(\frac{\sigma_{v0}}{\sigma'_{v0}}\right) rd \quad (1)$$

where CSR = Cyclic Stress Ratio, a_{max} = peak ground acceleration, g = gravitational acceleration, σ_{v0} = total vertical overburden stress, σ'_{v0} = effective vertical overburden stress and rd = stress reduction coefficient

The CSR value represents the cyclic seismic demand generated by earthquake shaking at different soil depths. In general, CSR increases with increasing seismic acceleration and overburden stress.

The cyclic resistance of soil against liquefaction (CSRL) was then estimated from CPT data using normalized cone resistance values and empirical correlations proposed by (Robertson and Wride, 1998) and updated by (Robertson and Cabal, 2022). The normalized cone resistance reflects soil density and stiffness, which control liquefaction resistance.

The liquefaction potential was evaluated by comparing CSR and CSRL values through the factor of safety (FS):

$$FS = \frac{CSRL}{CSR} \quad (2)$$

where $FS < 1.0$ indicates potentially liquefiable soil and $FS > 1.0$ indicates non-liquefiable or stable soil conditions.

In order to evaluate the liquefaction potential, this study used peak ground acceleration values of 0.15 g, 0.28 g, and 0.60 g. Subsequently, the evaluation of volumetric strain was conducted using the finite element method.

The CPT soundings were performed using a conventional mechanical cone penetration test (CPT) penetrometer with a maximum capacity of 2.5 tons. The tests were conducted by pushing the

cone into the ground at a constant penetration rate of approximately 20 mm/s, while continuously recording the cone tip resistance (qc) and sleeve friction (fs) with depth. The groundwater table at all three CPT locations was measured at approximately 1.0–1.5 m below the ground surface, reflecting the shallow coastal hydrogeological setting. The post-liquefaction volumetric strain analysis was carried out using two-dimensional finite element software (PLAXIS 2D). The subsurface stratigraphy at each CPT location was represented as a horizontally layered soil column using 15-noded triangular elements, with a refined mesh applied within the upper 15 m to capture the CPT-interpreted layer boundaries. Soil layers were modelled using the Mohr-Coulomb constitutive model, with unit weight, effective friction angle, and stiffness (Young's modulus) parameters estimated from the CPT cone resistance and soil behavior type index following the correlations of Robertson and Cabal (2022). Standard fixities were applied at the model boundaries, with full fixity at the base and horizontal restraint along the vertical side boundaries, while the phreatic level was set according to the field-measured groundwater depth. The initial in-situ stress state was generated using the K0-procedure prior to the application of the equivalent seismic loading corresponding to each peak ground acceleration scenario (0.15 g, 0.28 g, and 0.60 g), after which the resulting volumetric strain was extracted for each soil layer and correlated with the corresponding safety factor.

RESULTS AND DISCUSSION

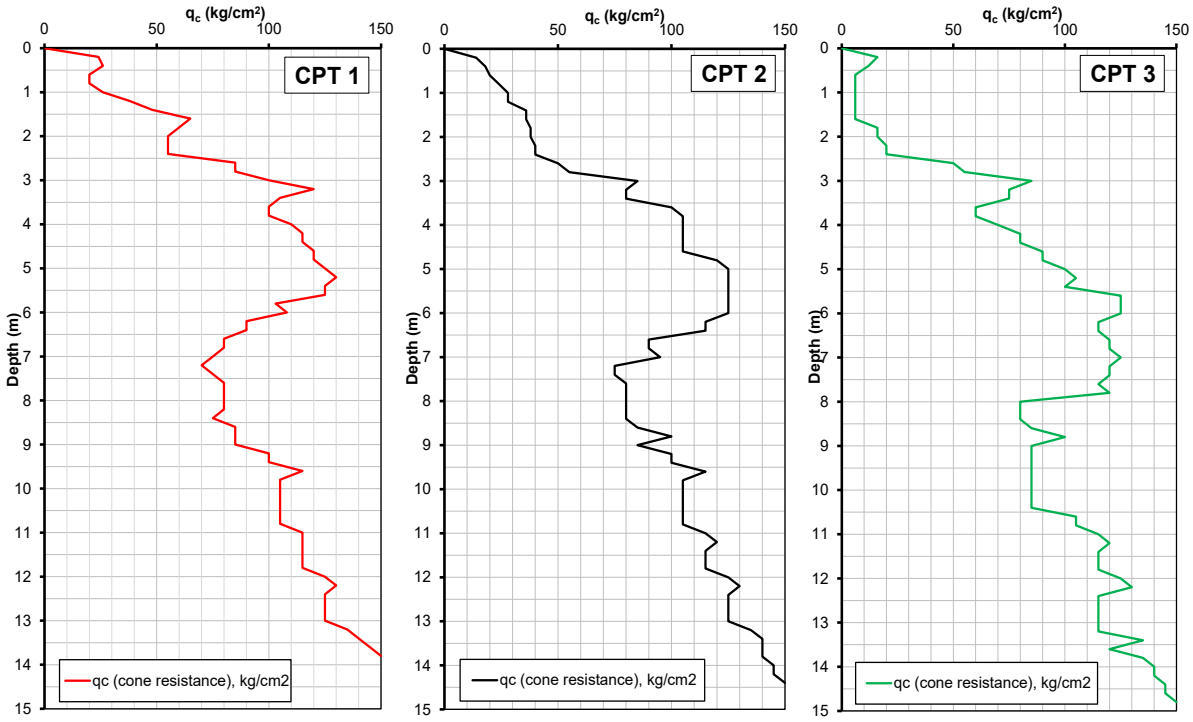
Figure 2 presents the cone resistance profiles and interpreted soil stratigraphy obtained from three Cone Penetration Test (CPT). The CPT results indicate significant vertical and lateral variability in subsurface soil conditions within the investigated coastal deposits. In general, the subsurface profile is dominated by sandy silt, silty sand, loose sand, and localized clay layers, which are commonly associated with young coastal alluvial deposits.

At CPT-1, the upper soil layer from approximately 1–2 m depth is characterized by sandy silt to clayey silt deposits with relatively low cone resistance values, indicating soft to medium consistency soils. Between depths of approximately 2–6 m, the profile is dominated by sand to silty sand layers, where an increase in cone resistance values suggests relatively denser granular material. However, the interval between 7–10 m depth again exhibits sandy silt to clayey silt deposits with lower cone resistance, indicating the presence of compressible fine-grained materials. At deeper depths, particularly below 12 m, the soil profile transitions into sand deposits with higher cone resistance values, reflecting denser soil conditions.

The CPT-2 profile shows relatively similar stratigraphic characteristics. The shallow layer between 1–3 m depth consists predominantly of sandy silt to clayey silt with low to moderate cone resistance values. This layer is underlain by sand to silty sand deposits extending to approximately 7 m depth, where cone resistance values increase significantly, indicating medium-dense to dense granular soils. From approximately 7–9 m depth, finer-grained deposits reappear with lower cone resistance values before transitioning into thicker sand layers below 9 m depth. The deeper sandy deposits exhibit progressively increasing cone resistance values, suggesting improved soil density and stiffness with depth.

On the other hand, CPT-3 demonstrates slightly different near-surface conditions compared with CPT-1 and CPT-2. A thin clay layer is identified within the upper 1–2 m depth interval, characterized by very low cone resistance values. Below this layer, sandy silt to clayey silt deposits dominate until approximately 6 m depth, followed by sand to silty sand layers between 6–8 m depth. The soil profile then transitions back into sandy silt to clayey silt deposits at intermediate depths before reaching dense sand deposits below approximately 12 m depth. The cone resistance values within the deeper sand layers increase substantially, indicating relatively dense granular materials.

The liquefaction potential assessment based on the CPT 1 results was conducted using three peak ground acceleration scenarios, namely 0.15 g, 0.28 g and 0.60 g, to evaluate the variation of cyclic shear stress induced by earthquake loading and the corresponding liquefaction resistance of the soil layers. The comparison between Cyclic Stress Ratio (CSR) and Cyclic Stress Ratio Required for Liquefaction (CSRL) provides a clear indication of the potential liquefaction susceptibility at different depths.



Depth (m)	Cone Penetration (CPT) 1	Cone Penetration (CPT) 2	Cone Penetration (CPT) 3
	Soil Type		
1.00	Sandy silt to clayey silt	Sandy silt to clayey silt	Clay
2.00			
3.00	Sand to silty sand		Sandy silt to clayey silt
4.00		Sand to silty sand	
5.00			
6.00			
7.00	Sandy silt to clayey silt		Sand to silty sand
8.00		Sandy silt to clayey silt	
9.00			
10.00		Sand to silty sand	Sandy silt to clayey silt
11.00	Sand to silty sand		
12.00			
13.00	Sand		Sand
14.00		Sand	
15.00			

Figure 2. The Soil Stratigraphy based on the CPT tests.

For the seismic loading condition 0.15 g, the induced cyclic shear stress remains relatively low throughout the investigated depth profile. The CSR values are consistently lower than the CSRL values, indicating that the soil deposits possess sufficient resistance against earthquake-induced liquefaction. Then, under the intermediate seismic scenario 0.28 g, the cyclic shear stress increases significantly with depth. The CSR curve approaches the CSRL boundary within several soil layers, particularly at depths ranging from approximately 6–10 m. This behavior indicates an increase in liquefaction susceptibility due to higher earthquake-induced shear stresses. Several loose to medium-dense sandy layers appear to exhibit marginal stability conditions where the applied cyclic stress nearly equals the liquefaction resistance. Consequently, localized liquefaction may potentially occur within these critical layers during strong seismic events of moderate intensity. For the highest seismic scenario 0.60 g, the CSR values substantially exceed the CSRL values across most investigated depths. This condition clearly indicates a high liquefaction potential throughout the subsurface profile. The most critical zones are identified within the depth interval of approximately 3–13 m, where the earthquake-induced cyclic stress is considerably greater than the soil resistance. The significant separation between CSR and CSRL demonstrates that the soil layers are unable to sustain

the imposed cyclic loading, resulting in a high probability of excess pore water pressure generation and subsequent strength degradation (see Figure 3). This behavior is characteristic of loose saturated sandy deposits subjected to severe seismic loading (Robertson et al, 2022; Robertson et al, 1998).

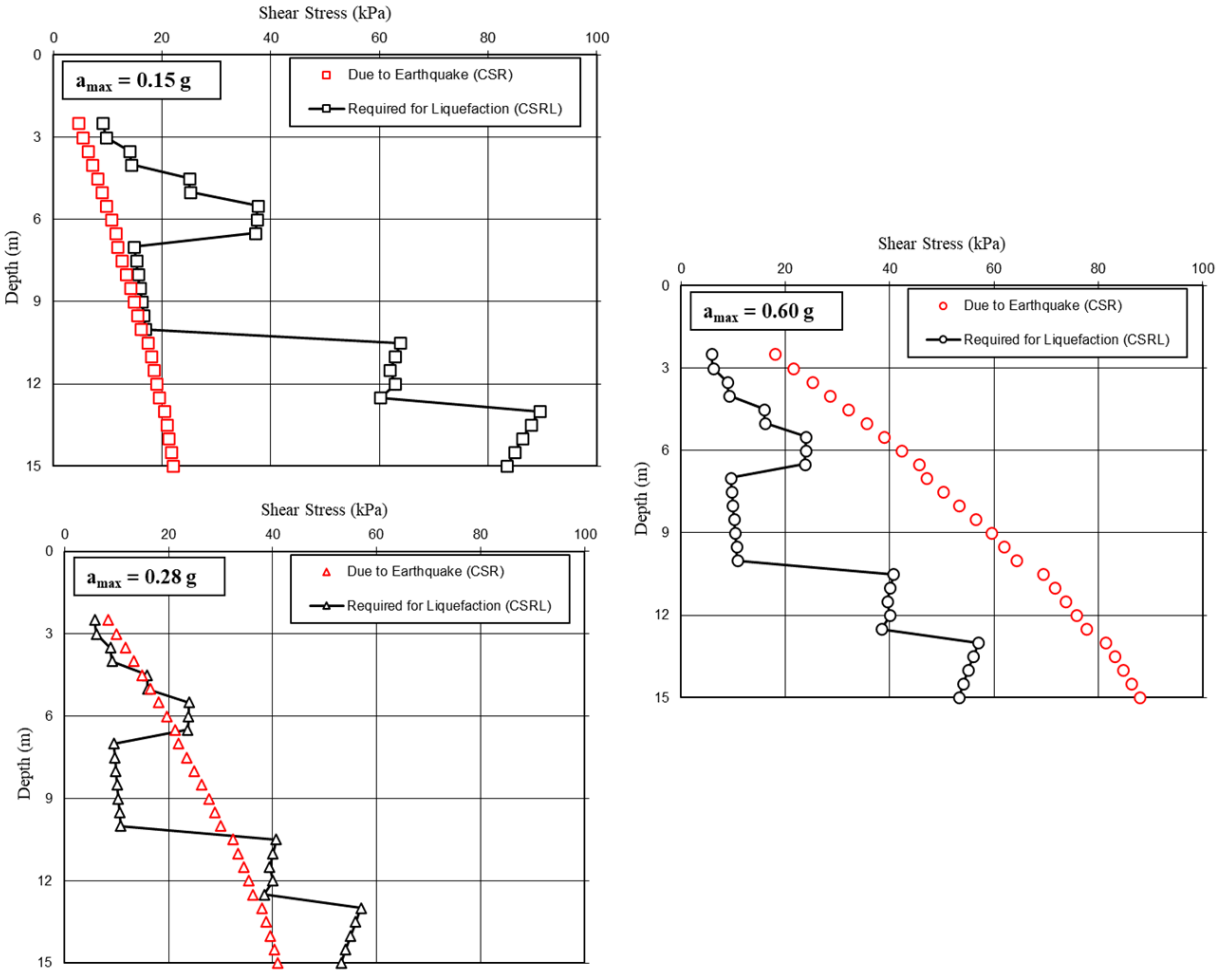


Figure 3. The comparison between Cyclic Stress Ratio (CSR) and Cyclic Stress Ratio Required for Liquefaction (CSRL) CPT 1.

In order to provide a comprehensive assessment of the liquefaction susceptibility at CPT-1, CPT-2, and CPT-3 locations, the safety factor (SF) against liquefaction was calculated for each investigated soil layer. The calculated results are presented in Figure 4.

For the low seismic loading condition 0.15 g, the majority of the investigated soil layers exhibit safety factor values significantly greater than 1.0 across all CPT soundings. The SF values generally range between 1.2 and 3.8, indicating adequate liquefaction resistance under moderate earthquake excitation. Higher SF values are predominantly observed within the depth intervals of approximately 3–6 m and 10–15 m, suggesting relatively dense soil conditions with sufficient cyclic resistance. Although several layers at depths around 8–10 m show SF values approaching unity, the overall subsurface profile remains stable and demonstrates low liquefaction susceptibility under this seismic scenario.

Under the intermediate seismic loading condition 0.28 g, a substantial reduction in safety factor values is observed throughout the soil profile. Several layers within depths of approximately 6–10 m and 13–15 m exhibit SF values close to or slightly below 1.0, particularly in CPT-1 and CPT-3. This condition indicates that the cyclic shear stresses generated by the earthquake loading begin to exceed the liquefaction resistance of the soil. The reduction in SF values suggests that loose to medium-dense sandy deposits become increasingly vulnerable to excess pore water pressure

generation during seismic shaking. Consequently, localized liquefaction is likely to occur within these critical depth intervals during moderate-to-strong earthquake events.

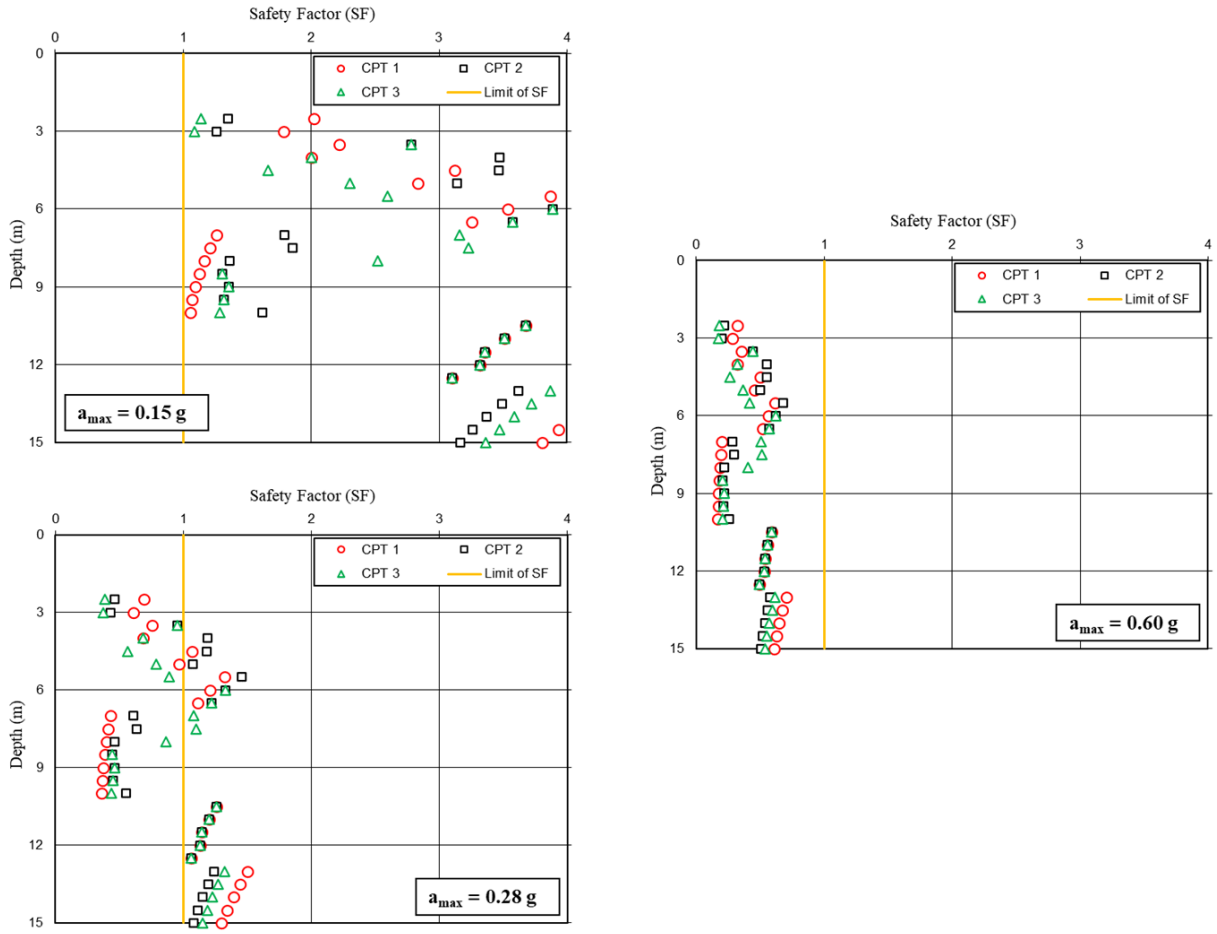


Figure 4. The comparison between safety factor (SF) and soil depth.

Furthermore, for the highest seismic loading scenario 0.60 g, the safety factor values decrease dramatically across nearly all investigated depths and CPT locations. Most SF values fall below the critical threshold of 1.0, indicating widespread liquefaction susceptibility throughout the subsurface deposits. The critical zones are particularly concentrated between depths of approximately 3–15 m, where the soil layers exhibit very low resistance against cyclic loading. This behavior demonstrates that severe earthquake excitation substantially increases the potential for liquefaction-induced soil failure, including excessive settlement, lateral spreading (Bartlett and Youd, 1995), and loss of bearing capacity. The consistent reduction in SF values across CPT-1, CPT-2, and CPT-3 also indicates relatively uniform vulnerable soil conditions within the study area.

The safety factor analysis demonstrates a strong correlation between increasing peak ground acceleration and decreasing liquefaction resistance. The results confirm that the investigated coastal sediments remain relatively stable under low seismic loading but become progressively unstable as earthquake intensity increases. These findings are consistent with previous studies indicating that saturated loose sandy deposits in coastal environments are highly sensitive to cyclic loading and are particularly vulnerable during strong seismic events (Robertson et al, 2022; Robertson et al, 1998).

Furthermore, based on the finite element method, the relationship between the average safety factor (SF) and volumetric strain (εv) demonstrates a clear inverse correlation, as presented in Figure 5. The results indicate that decreasing safety factor values are associated with increasing volumetric strain, confirming that soil layers with lower liquefaction resistance tend to experience greater post-liquefaction deformation. The regression analysis yields a coefficient of determination ($R^2 = 0.7761$), indicating a strong correlation between liquefaction susceptibility and volumetric strain behavior.

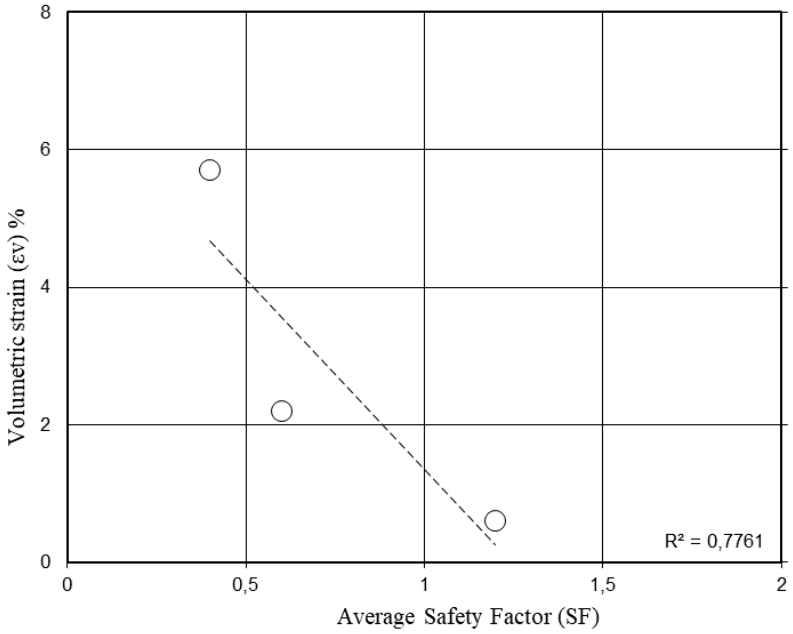


Figure 5. The relationship between the average safety factor (SF) and volumetric strain (εv).

The safety factor ranges obtained in this study are broadly consistent with the coastal Padang findings of Mase (2017), where loose sandy layers were also shown to become unstable once peak ground acceleration exceeded approximately 0.2-0.3 g, and with the microzonation results of Tohari (2020) for the wider West Sumatera coast. The pattern of decreasing SF with depth and increasing acceleration is also in line with the CPT-based triggering framework of (Robertson and Cabal, 2022) and the probabilistic case-history database of (Moss et al, 2006), and is qualitatively similar to liquefaction behavior documented for saturated coastal sands following major subduction-zone earthquakes in Japan, Chile, and New Zealand (Green et al., 2014; Cubrinovski et al., 2011), where loose, shallow-groundwater deposits close to the shoreline have repeatedly proven to be the most vulnerable. This consistency with independent datasets and methods supports the reliability of the CPT-CSR/CRR approach used here, while the additional volumetric strain analysis extends these earlier triggering-only studies toward a deformation-based hazard characterization.

Several limitations of this study should be acknowledged. First, the assessment is based on only three CPT soundings, which, while sufficient to characterize the general stratigraphic pattern along the investigated segment, cannot fully capture lateral heterogeneity across the broader southern coastal zone. Second, the simplified Seed and Idriss procedure used to compute CSR assumes one-dimensional, vertically propagating shear waves and a level ground surface, and does not explicitly account for near-fault directivity effects or the specific source characteristics of a future Sunda megathrust rupture. Third, the finite element analysis employed a Mohr-Coulomb constitutive model, which, despite being computationally efficient and adequate for estimating overall volumetric strain trends, does not capture the full cyclic pore-pressure generation and dilatancy behavior that more advanced effective-stress models such as UBCSAND or PM4Sand (Boulanger and Ziotopoulou, 2015) can represent. Finally, the groundwater table was assumed to be constant at the measured field depth, whereas seasonal and tidal fluctuations in this shoreline setting could locally increase or decrease liquefaction susceptibility. Future work should therefore incorporate additional CPT and borehole data, advanced cyclic constitutive models, and monitored groundwater variability to refine the hazard estimates presented here.

Given the widespread liquefaction susceptibility identified under moderate-to-strong seismic loading, ground improvement should be considered for coastal defense and public infrastructure planned within the investigated area. Depending on structural loads, layer depth, and cost constraints, suitable mitigation measures include vibro-compaction and stone columns for loose sandy layers at shallow-to-moderate depth, deep soil mixing for zones containing softer silty layers, pile foundations extending below the critical liquefiable depth for structures sensitive to settlement,

and preloading with vertical drains where construction schedules permit staged ground improvement. Selection among these options should be guided by site-specific geotechnical investigation and cost-benefit analysis for each planned facility.

CONCLUSION

This study evaluated the liquefaction potential of coastal deposits in the southern coastal area of West Sumatera using Cone Penetration Test (CPT). The results demonstrate that seismic intensity has a significant influence on liquefaction susceptibility. Under the low seismic loading condition 0.15 g, most soil layers exhibited safety factors values greater than 1.0, indicating stable ground conditions and low liquefaction potential. However, under intermediate seismic loading 0.28 g, several soil layers, particularly within the depth range of approximately 6–10 m, showed SF values approaching unity, indicating marginal stability and localized liquefaction susceptibility. For the highest seismic scenario (0.60 g), the CSR values exceeded the liquefaction resistance across most investigated depths, resulting in SF values below 1.0 and indicating a high probability of liquefaction occurrence. The analysis also revealed that the investigated coastal deposits, which are predominantly composed of loose saturated sandy soils, are highly vulnerable to strong cyclic loading. The volumetric strain evaluation further confirmed that lower safety factor values correspond to higher post-liquefaction deformation potential. A strong inverse correlation between average SF and volumetric strain was obtained, with a coefficient determination of $R^2 = 0.7761$, demonstrating that decreasing liquefaction resistance significantly increases the risk of ground deformation. Overall, the integration of CPT-based liquefaction analysis and finite element modelling provides a comprehensive approach for evaluating seismic ground response in coastal environments. The findings of this study emphasize the necessity of considering liquefaction mitigation strategies and ground improvement techniques for infrastructure development in earthquake-prone coastal regions, particularly in areas characterized by loose granular sediments and high groundwater conditions.

The main scientific contribution of this study is the coupling of empirical CPT-based triggering analysis with finite element modelling of post-liquefaction volumetric strain for a previously uninvestigated coastal segment, which extends prior triggering-only assessments (e.g., Mase. L, 2017; Tohari. A, 2020) toward a deformation-based hazard characterization directly relevant to coastal defense infrastructure design. Methodologically, the study demonstrates a practical workflow for linking cone resistance profiles, an empirical safety factor, and finite element-derived ground deformation using widely available soil parameters. These findings can support the selection of appropriate ground-improvement strategies and foundation types for defense and civilian infrastructure planned along this coastline. Nonetheless, the results are constrained by the limited number of CPT points, the assumptions embedded in the simplified Seed and Idriss procedure, the use of a Mohr-Coulomb constitutive model rather than an advanced cyclic soil model, and the assumption of a constant groundwater level; future studies incorporating additional subsurface investigations, advanced constitutive models, and groundwater monitoring are recommended to refine these estimates.

AUTHOR CONTRIBUTIONS

O.A.P.: Conceptualization, data curation, funding acquisition, investigation, methodology, visualization, writing –original, and writing - review & editing. H.M.: Investigation & formal analysis. F.N.: Investigation & review.

CONFLICT OF INTEREST

The authors declare that they have no known competing financial interests or personal relationships that could have appeared to influence the work reported in this paper.

REFERENCES

Andrus, R. D., & Stokoe, K. H. (2000). Liquefaction resistance of soils from shear-wave velocity. Journal of Geotechnical and Geoenvironmental Engineering, 126(11), 1015–1025. https://doi.org/10.1061/(ASCE)1090-0241(2000)126:11(1015)

Bartlett, S. F., & Youd, T. L. (1995). Empirical prediction of liquefaction-induced lateral spread. Journal of Geotechnical Engineering, 121(4), 316–329. https://doi.org/10.1061/(ASCE)0733-9410(1995)121:4(316)

Boulanger, R. W., & Idriss, I. M. (2014). CPT and SPT based liquefaction triggering procedures. Center for Geotechnical Modeling, University of California, Davis.

Boulanger, R. W., & Idriss, I. M. (2016). CPT-based liquefaction triggering procedure. Journal of Geotechnical and Geoenvironmental Engineering, 142(2), 04015065. https://doi.org/10.1061/(ASCE)GT.1943-5606.0001388

Boulanger, R. W., & Ziotopoulou, K. (2015). PM4Sand (version 3): A sand plasticity model for earthquake engineering applications. Report No. UCD/CGM-15/01, Center for Geotechnical Modeling, University of California, Davis.

Bray, J. D., & Macedo, J. (2017). 6th Ishihara Lecture: Simplified procedure for estimating liquefaction-induced building settlement. Soil Dynamics and Earthquake Engineering, 102, 215–231. https://doi.org/10.1016/j.soildyn.2017.08.026

Bray, J. D., & Sancio, R. B. (2006). Assessment of the liquefaction susceptibility of fine-grained soils. Journal of Geotechnical and Geoenvironmental Engineering, 132(9), 1165–1177. https://doi.org/10.1061/(ASCE)1090-0241(2006)132:9(1165)

Cetin, K. O., Seed, R. B., Der Kiureghian, A., Tokimatsu, K., Harder Jr., L. F., Kayen, R. E., & Moss, R. E. S. (2004). Standard penetration test-based probabilistic and deterministic assessment of seismic soil liquefaction potential. Journal of Geotechnical and Geoenvironmental Engineering, 130(12), 1314–1340. https://doi.org/10.1061/(ASCE)1090-0241(2004)130:12(1314)

Cubrinovski, M., Bray, J. D., Taylor, M., Giorgini, S., Bradley, B., Wotherspoon, L., & Zupan, J. (2011). Soil liquefaction effects in the central business district during the February 2011 Christchurch earthquake. Seismological Research Letters, 82(6), 893–904. https://doi.org/10.1785/gssrl.82.6.893

Das, B. M., & Sobhan, K. (2018). Principles of geotechnical engineering (9th ed.). Cengage Learning.

Geyin, M., & Maurer, B. W. (2021). Evaluation of a cone penetration test thin-layer correction procedure in the context of global liquefaction model performance. Engineering Geology, 291, 106221. https://doi.org/10.1016/j.enggeo.2021.106221

Green, R. A., Cubrinovski, M., Cox, B., Wood, C., Wotherspoon, L., Bradley, B., & Maurer, B. (2014). Select liquefaction case histories from the 2010–2011 Canterbury earthquake sequence. Earthquake Spectra, 30(1), 131–153. https://doi.org/10.1193/030713EQS066M

Hall, R. (2012). Late Jurassic–Cenozoic reconstructions of the Indonesian region and the Indian Ocean. Tectonophysics, 570–571, 1–41. https://doi.org/10.1016/j.tecto.2012.04.021

Idriss, I. M., & Boulanger, R. W. (2006). Semi-empirical procedures for evaluating liquefaction potential during earthquakes. Soil Dynamics and Earthquake Engineering, 26(2–4), 115–130. https://doi.org/10.1016/j.soildyn.2004.11.023

Idriss, I. M., & Boulanger, R. W. (2008). Soil liquefaction during earthquakes. Earthquake Engineering Research Institute.

Ishihara, K. (1993). Liquefaction and flow failure during earthquakes. Geotechnique, 43(3), 351–451. https://doi.org/10.1680/geot.1993.43.3.351

Ishihara, K., & Yoshimine, M. (1992). Evaluation of settlements in sand deposits following liquefaction during earthquakes. Soils and Foundations, 32(1), 173–188. https://doi.org/10.3208/sandf1972.32.173

Iwasaki, T., Tatsuoka, F., Tokida, K., & Yasuda, S. (1978). A practical method for assessing soil liquefaction potential based on case studies at various sites in Japan. Proceedings of the 2nd International Conference on Microzonation, San Francisco, 885–896.

Juang, C. H., Fang, S. Y., & Khor, E. H. (2006). First-order reliability method for probabilistic liquefaction triggering analysis using CPT. Journal of Geotechnical and Geoenvironmental Engineering, 132(3), 337–350. https://doi.org/10.1061/(ASCE)1090-0241(2006)132:3(337)

Kayen, R., Moss, R. E. S., Thompson, E. M., Seed, R. B., Cetin, K. O., Der Kiureghian, A., Tanaka, Y., & Tokimatsu, K. (2013). Shear-wave velocity-based probabilistic and deterministic assessment of seismic soil liquefaction potential. Journal of Geotechnical and Geoenvironmental Engineering, 139(3), 407–419. https://doi.org/10.1061/(ASCE)GT.1943-5606.0000743

Kramer, S. L. (1996). Geotechnical earthquake engineering. Prentice Hall.

Lunne, T., Robertson, P. K., & Powell, J. J. M. (1997). Cone penetration testing in geotechnical practice. Blackie Academic & Professional.

Mase, L. Z. (2017). Liquefaction potential analysis along coastal area of Padang due to earthquake loading. International Journal of GEOMATE, 13(35), 134–141. https://doi.org/10.21660/2017.35.2736

Moss, R. E. S., Seed, R. B., Kayen, R. E., Stewart, J. P., Der Kiureghian, A., & Cetin, K. O. (2006). CPT-based probabilistic and deterministic assessment of in situ seismic soil liquefaction potential. Journal of Geotechnical and Geoenvironmental Engineering, 132(8), 1032–1051. https://doi.org/10.1061/(ASCE)1090-0241(2006)132:8(1032)

Natawidjaja, D. H., & Triyoso, W. (2007). The Sumatran fault zone – from source to hazard. Journal of Earthquake and Tsunami, 1(1), 21–47. https://doi.org/10.1142/S1793431107000031

Putra, O. A., et al. (2020). Effect of soil structure disturbance on the shear strength of black volcanic ash soil. E3S Web of Conferences, 156, 02004. https://doi.org/10.1051/e3sconf/202015602004

Robertson, P. K. (2009). Interpretation of cone penetration tests – a unified approach. Canadian Geotechnical Journal, 46(11), 1337–1355. https://doi.org/10.1139/T09-065

Robertson, P. K., & Cabal, K. L. (2022). Guide to cone penetration testing for geotechnical engineering (7th ed.). Gregg Drilling & Testing, Inc.

Robertson, P. K., & Wride, C. E. (1998). Evaluating cyclic liquefaction potential using the cone penetration test. Canadian Geotechnical Journal, 35(3), 442–459. https://doi.org/10.1139/t98-017

Seed, H. B., & Idriss, I. M. (1971). Simplified procedure for evaluating soil liquefaction potential. Journal of the Soil Mechanics and Foundations Division, 97(9), 1249–1273. https://doi.org/10.1061/JSFEAQ.0001662

Seed, H. B., Tokimatsu, K., Harder, L. F., & Chung, R. M. (1985). Influence of SPT procedures in soil liquefaction resistance evaluations. Journal of Geotechnical Engineering, 111(12), 1425–1445. https://doi.org/10.1061/(ASCE)0733-9410(1985)111:12(1425)

Seed, R. B., Cetin, K. O., Moss, R. E. S., Kammerer, A. M., Wu, J., Pestana, J. M., Riemer, M. F., Sancio, R. B., Bray, J. D., Kayen, R. E., & Faris, A. (2003). Recent advances in soil liquefaction engineering and seismic site response evaluation. Proceedings of the 4th International Conference on Recent Advances in Geotechnical Earthquake Engineering and Soil Dynamics, San Diego, California.

Sieh, K., & Natawidjaja, D. (2000). Neotectonics of the Sumatran fault, Indonesia. Journal of Geophysical Research, 105(B12), 28295–28326. https://doi.org/10.1029/2000JB900120

Tohari, A. (2020). Seismic microzonation of soil amplification and liquefaction for Padang City. E3S Web of Conferences, 156, 02008. https://doi.org/10.1051/e3sconf/202015602008

Tokimatsu, K., & Seed, H. B. (1987). Evaluation of settlements in sands due to earthquake shaking. Journal of Geotechnical Engineering, 113(8), 861–878. https://doi.org/10.1061/(ASCE)0733-9410(1987)113:8(861)

Towhata, I. (2008). Geotechnical earthquake engineering. Springer. https://doi.org/10.1007/978-3-540-35783-4

Wang, J. S., Hwang, J. H., Deng, Y. C., et al. (2023). Model uncertainties of SPT, CPT, and Vs-based simplified methods for soil liquefaction assessment. Bulletin of Engineering Geology and the Environment, 82, 260. https://doi.org/10.1007/s10064-023-03300-6

Yegian, M. K., & Vitelli, J. F. (1981). Relating local geology and seismicity to regional liquefaction potential. Journal of Geotechnical Engineering Division, 107(2), 145–158.

Youd, T. L., Idriss, I. M., Andrus, R. D., Arango, I., Castro, G., Christian, J. T., Dobry, R., Finn, W. D. L., Harder Jr., L. F., Hynes, M. E., Ishihara, K., Koester, J. P., Liao, S. S. C., Marcuson III, W. F., Martin, G. R., Mitchell, J. K., Moriwaki, Y., Power, M. S., Robertson, P. K., Seed, R. B., & Stokoe II, K. H. (2001). Liquefaction resistance of soils: Summary report from the 1996 NCEER and 1998 NCEER/NSF workshops on evaluation of liquefaction resistance of soils. Journal of Geotechnical and Geoenvironmental Engineering, 127(10), 817–833. https://doi.org/10.1061/(ASCE)1090-0241(2001)127:10(817)

Zhang, G., Robertson, P. K., & Brachman, R. W. I. (2002). Estimating liquefaction-induced ground settlements from CPT for level ground. Canadian Geotechnical Journal, 39(5), 1168–1180. https://doi.org/10.1139/t02-047